

Supporting Data

Strain-induced Dirac cone-like electronic structures and semiconductor-semimetal transition in graphdiyne

Hui-Juan Cui¹, Xian-Lei Sheng², Qing-Bo Yan³, Qing-Rong Zheng¹, and Gang Su^{1*}

¹*School of Physics, University of Chinese Academy of Sciences, P. O. Box 4588, Beijing 100049, China*

²*Beijing National Laboratory for Condensed Matter Physics, Institute of Physics, Chinese Academy of Sciences, P. O. Box 4588, Beijing 100190, China*

³*College of Materials Science and Opto-Electronic Technology, University of Chinese Academy of Sciences, P. O. Box 4588, Beijing 100049, China*

1. Tight-binding model for graphdiyne under biaxial strain and no strain

For convenience of characterizing the hopping matrix, we label each carbon atom by a number as in Fig. S1.

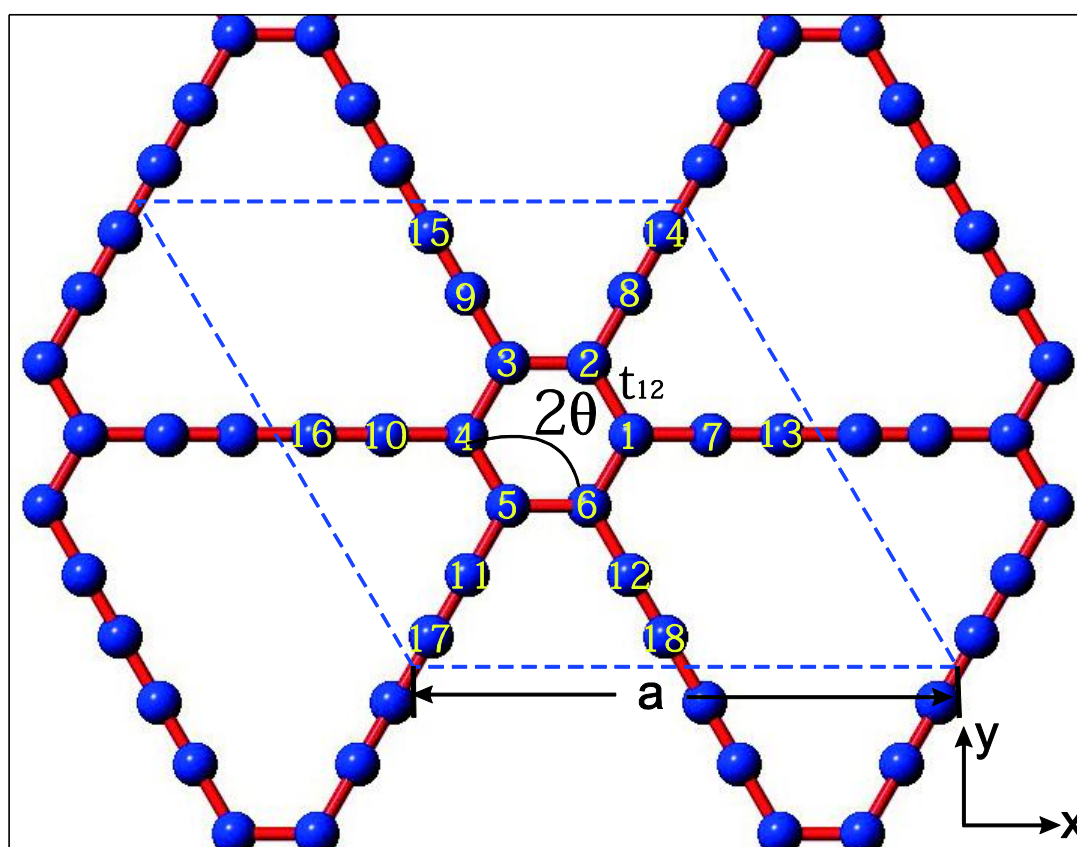


Fig. S1. Schematic structure of graphdiyne, and the label of carbon atoms in a unit cell (the parallelogram) for the hopping matrix of Hamiltonian. $t_{i,j}$ is defined as the hopping amplitude between site i and site j labeled by numbers (from 1 to 18).

The Hamiltonian can be written as in Wannier representation

$$\hat{H} = \sum_{\vec{r}, \vec{\delta}} \hat{\psi}_{\vec{r}}^{\dagger} T_{\vec{\delta}} \hat{\psi}_{\vec{r}+\vec{\delta}} \quad (1)$$

where $\hat{\psi} = (\hat{c}_{\vec{r},1}, \hat{c}_{\vec{r},2}, \hat{c}_{\vec{r},3}, \hat{c}_{\vec{r},4} \cdots \hat{c}_{\vec{r},17}, \hat{c}_{\vec{r},18})$, and $\delta = \{\vec{e}_x, \vec{e}_y, -\vec{e}_x, -\vec{e}_y, 0\}$. After making Fourier transform, we have

$$\hat{H} = \hat{\psi}_k^{\dagger} H_k \hat{\psi}_k \quad (2)$$

with

$$H'_k = \begin{pmatrix} 0 & t_1 & 0 & 0 & 0 & t_1 & t_2 & 0 & 0 & 0 & 0 & 0 & 0 & 0 & 0 & 0 & 0 & 0 & 0 \\ t_1 & 0 & t'_1 & 0 & 0 & 0 & 0 & t'_2 & 0 & 0 & 0 & 0 & 0 & 0 & 0 & 0 & 0 & 0 & 0 \\ 0 & t'_1 & 0 & t_1 & 0 & 0 & 0 & 0 & t'_2 & 0 & 0 & 0 & 0 & 0 & 0 & 0 & 0 & 0 & 0 \\ 0 & 0 & t_1 & 0 & t_1 & 0 & 0 & 0 & 0 & t_2 & 0 & 0 & 0 & 0 & 0 & 0 & 0 & 0 & 0 \\ 0 & 0 & 0 & t_1 & 0 & t'_1 & 0 & 0 & 0 & 0 & t'_2 & 0 & 0 & 0 & 0 & 0 & 0 & 0 & 0 \\ t_1 & 0 & 0 & 0 & t'_1 & 0 & 0 & 0 & 0 & 0 & 0 & t'_2 & 0 & 0 & 0 & 0 & 0 & 0 & 0 \\ t_2 & 0 & 0 & 0 & 0 & 0 & 0 & 0 & 0 & 0 & 0 & 0 & t_3 & 0 & 0 & 0 & 0 & 0 & 0 \\ 0 & t'_2 & 0 & 0 & 0 & 0 & 0 & 0 & 0 & 0 & 0 & 0 & 0 & t'_3 & 0 & 0 & 0 & 0 & 0 \\ 0 & 0 & t'_2 & 0 & 0 & 0 & 0 & 0 & 0 & 0 & 0 & 0 & 0 & 0 & t'_3 & 0 & 0 & 0 & 0 \\ 0 & 0 & 0 & t_2 & 0 & 0 & 0 & 0 & 0 & 0 & 0 & 0 & 0 & 0 & 0 & t_3 & 0 & 0 & 0 \\ 0 & 0 & 0 & 0 & t'_2 & 0 & 0 & 0 & 0 & 0 & 0 & 0 & 0 & 0 & 0 & 0 & 0 & t'_3 & 0 \\ 0 & 0 & 0 & 0 & 0 & t'_2 & 0 & 0 & 0 & 0 & 0 & 0 & 0 & 0 & 0 & 0 & 0 & 0 & t'_3 \\ 0 & 0 & 0 & 0 & 0 & 0 & t_3 & 0 & 0 & 0 & 0 & 0 & 0 & 0 & 0 & t_4 e^{2ik_x \cos \theta} & 0 & 0 & 0 \\ 0 & 0 & 0 & 0 & 0 & 0 & 0 & t'_3 & 0 & 0 & 0 & 0 & 0 & 0 & 0 & 0 & t_4 e^{i(k_x \cos \theta + k_y \sin \theta)} & 0 & 0 \\ 0 & 0 & 0 & 0 & 0 & 0 & 0 & 0 & t'_3 & 0 & 0 & 0 & 0 & 0 & 0 & 0 & 0 & 0 & t_4 e^{i(-k_x \cos \theta + k_y \sin \theta)} \\ 0 & 0 & 0 & 0 & 0 & 0 & 0 & 0 & 0 & t_3 & 0 & 0 & t_4 e^{-2ik_x \cos \theta} & 0 & 0 & 0 & 0 & 0 & 0 \\ 0 & 0 & 0 & 0 & 0 & 0 & 0 & 0 & 0 & 0 & t'_3 & 0 & 0 & 0 & 0 & 0 & 0 & 0 & 0 \\ 0 & 0 & 0 & 0 & 0 & 0 & 0 & 0 & 0 & 0 & 0 & 0 & 0 & t_4 e^{i(-k_x \cos \theta - k_y \sin \theta)} & 0 & 0 & 0 & 0 & 0 \\ 0 & 0 & 0 & 0 & 0 & 0 & 0 & 0 & 0 & 0 & 0 & t'_3 & 0 & 0 & 0 & 0 & 0 & 0 & 0 \\ 0 & 0 & 0 & 0 & 0 & 0 & 0 & 0 & 0 & 0 & 0 & 0 & 0 & 0 & t_4 e^{i(k_x \cos \theta - k_y \sin \theta)} & 0 & 0 & 0 & 0 \end{pmatrix}$$

Table S2. The fitting values of t for different cases

strain	t_1 (eV)	t'_1 (eV)	t_2 (eV)	t'_2 (eV)	t_3 (eV)	t'_3 (eV)	t_4 (eV)	t'_4 (eV)	θ°
Armchair (5%)	-3.20	-3.11	-3.20	-3.37	-3.73	-3.81	-3.36	-3.52	58.13
Armchair (9%)	-3.02	-2.94	-2.49	-3.16	-3.27	-3.58	-2.69	-3.30	56.69
Armchair(15%)	-2.62	-2.49	-1.76	-2.76	-2.98	-3.12	-2.08	-2.88	54.54
Zigzag (5%)	-3.11	-3.19	-3.34	-2.89	-3.72	-3.64	-3.45	-3.30	62.87
Zigzag (9%)	-2.83	-2.99	-3.47	-2.87	-3.49	-3.70	-3.12	-2.85	62.90
Zigzag (15%)	-2.27	-1.98	-3.53	-2.47	-3.34	-3.53	-3.53	-2.30	64.42
Zigzag (19%)	-2.06	-3.66	-3.21	-2.25	-3.11	-3.27	-3.29	-1.91	65.79

3. The electron density change of the valence band maximum

The electron density change at the valence band maximum for different cases is shown in Fig. S2.

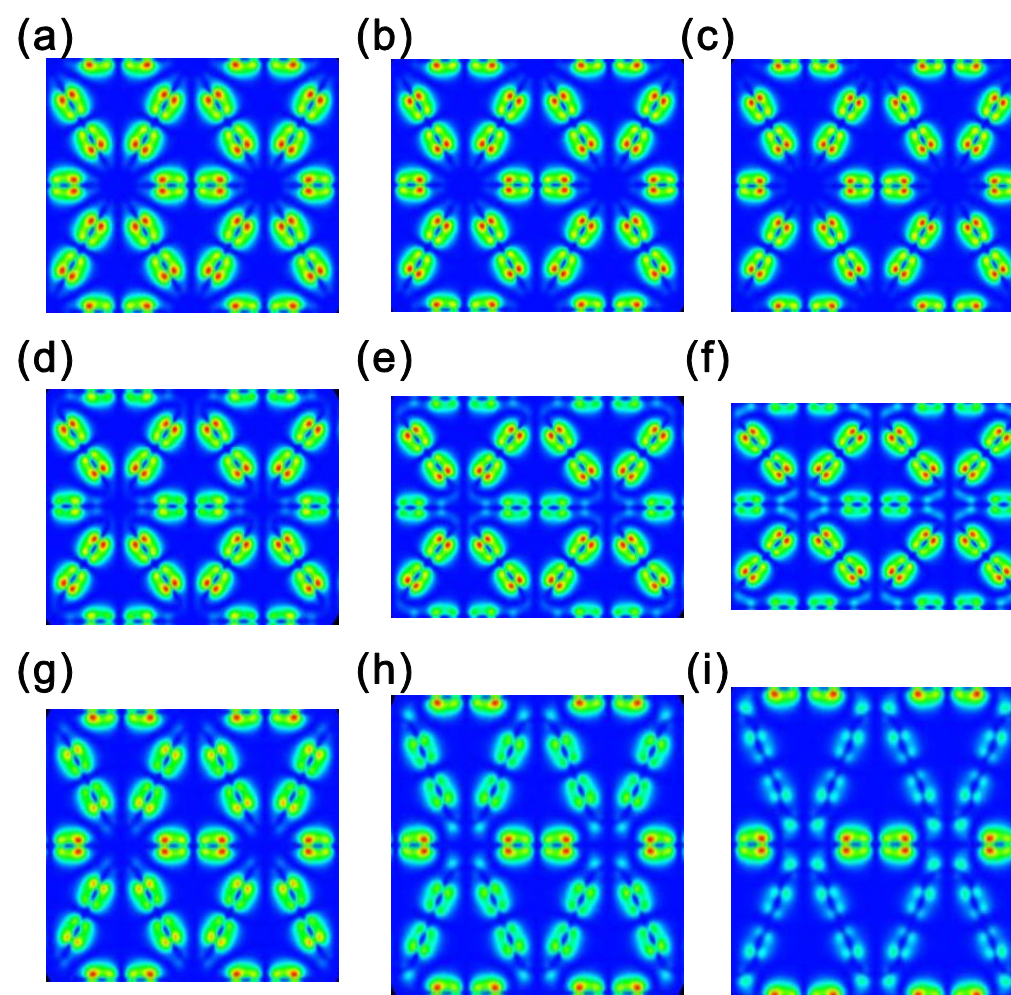


Fig. S2. The distribution of electron density of the valence band maximum under (a) no strain, biaxial strains of (b) 9% and (c) 15%, uniaxial tensile strains along the armchair direction with the strain of (d) 5%, (e) 9% and (f) 15%, and along the zigzag direction with the strain of (g) 5%, (h) 15% and (i) 19%.

4. The hole density change of the conduction band minimum

The hole density change at the conduction band minimum for different cases is shown in Fig. S3

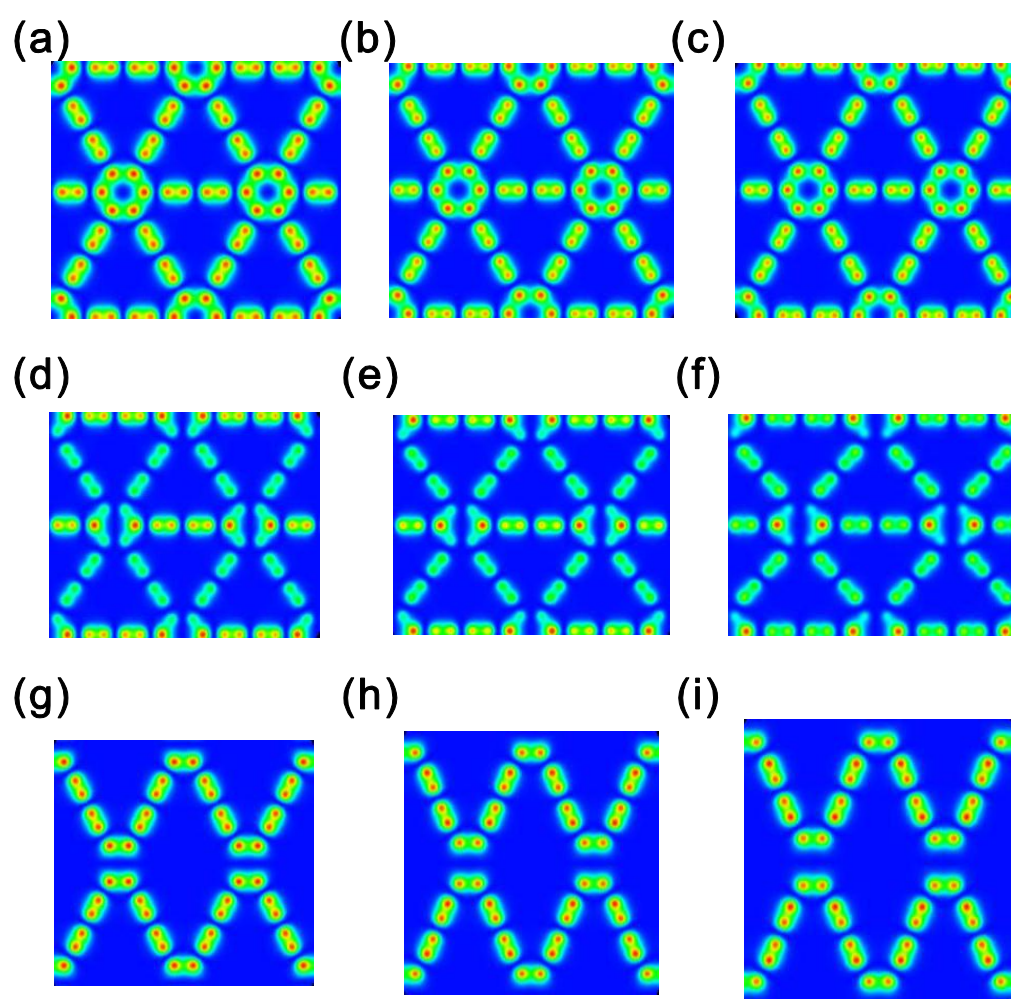


Fig. S3. The distribution of hole density of the conduction band minimum under (a) no strain, biaxial strains of (b) 9% and (c) 15%, uniaxial tensile strains along the armchair direction with the strain of (d) 5%, (e) 9% and (f) 15%, and along the zigzag direction with the strain of (g) 5%, (h) 15% and (i) 19%.